ISSN 0208-7774 TRIBOLOGIA 2/2022 p. 23–32
DOI: 10.5604/01.3001.0015.9720

Justyna KASIŃSKA[*], Monika MADEJ[**], Sławomir RUTKOWSKI[***]

EFFECTS OF RARE-EARTH METAL OXIDES ON THE TRIBOLOGICAL PROPERTIES OF PADDINGS FOR USE ON MINING MACHINE PARTS

WPŁYW DODATKÓW TLENKÓW METALI ZIEM RZADKICH NA WŁAŚCIWOŚCI TRIBOLOGICZNE NAPOIN STOSOWANYCH NA ELEMENTACH ROBOCZYCH MASZYN DLA GÓRNICTWA

Key words: pad welding, rare-earth metals, tribological wear, abrasive resistance.

Abstract: The article presents the results of research on pad welds made using consumables in the process of metal active gas welding (MAG) combined with plasma arc welding (PAW). The pad weld consisted of a buffer layer and a wear-resistant working layer. Cerium, yttrium and lanthanum oxides were added to the powders to modify the working (active) layer. The HV10 hardness and friction coefficient testing was followed by measuring wear tracks and determining wear indicators (maximum wear track depth and area). Yttrium oxide was found to have a remarkably beneficial effect on nickel-based pad welds. In the case of iron-based welds, the most favourable outcome was observed for lanthanum oxide.

Słowa kluczowe: napawanie, metale ziem rzadkich, zużycie tribologiczne, odporność na ścieranie.

Streszczenie: W artykule przedstawiono wyniki badań napoin wykonanych z wykorzystaniem materiałów spawalniczych metodą spawania łukowego elektrodą topliwą (MAG – metal active gas of welding) w połączeniu z napawaniem plazmowym (PAW – pasma arc welding). Napoina składała się z warstwy podkładowej (buforowej) oraz trudnościeralnej warstwy roboczej. Warstwę roboczą modyfikowano poprzez wprowadzanie do proszków tlenków ceru, itru i lantanu. Wykonane napoiny poddano pomiarom twardości HV10 oraz przeprowadzono testy tribologiczne, w których wyznaczono współczynnik tarcia. Następnie dokonano pomiarów śladów zużycia i zostały określone wskaźniki zużycia (maksymalna głębokość wytarcia, pole wytarcia). Wykazano korzystne oddziaływanie w szczególności tlenku itru dla napoin na osnowie niklu. W przypadku napoiny na osnowie żelaza najkorzystniejsze oddziaływanie odnotowano dla tlenku lantanu.

INTRODUCTION

Rare earth metals (REMs) have become a valuable resource for many technologies. Over the last decade, the application of REMs in electronics and nanotechnologies **[L. 1, 2]** further enhanced interest in REMs, which coincided with the development of the global market based on deposits in China. In the 20th century, REMs began to be used for steel and alloy modification for their beneficial effects on the mechanical properties and change of structure parameters, e.g., grain size reduction and the number and size of non-metallic inclusions **[L. 3–5]**. Due to their high tendency to oxidise,

[*] ORCID: 0000-0002-2225-0639. Kielce University of Technology, Faculty of Mechatronics and Mechanical Engineering, Tysiąclecia Państwa Polskiego Ave. 7, 25-314 Kielce, Poland.
[**] ORCID: 0000-0001-9892-9181. Kielce University of Technology, Faculty of Mechatronics and Mechanical Engineering, Tysiąclecia Państwa Polskiego Ave. 7, 25 314 Kielce, Poland.
[***] ORCID: 0000-0001-9966-6192. Przedsiębiorstwo Wielobranżowe T.S.A. Marcin Górski Sławomir Rutkowski, Przemysłowa Street 41, 37-450 Stalowa Wola, e-mail: srutkowski@pwtsa.pl; Rzeszow University of Technology, The Faculty of Mechanics and Technology, Kwiatkowskiego Street 4, 37-450 Stalowa Wola, Poland.

rare earth oxides, characterised by a high melting point, are used in sintered materials. In surface engineering, rare earth elements are widely applied in alloy coatings based on nickel **[L. 6, 7]** and iron **[L. 8]**. Their excellent tribological, anti-corrosive and mechanical properties **[L. 9–14]** find applications in the processes of laser surfacing, thermal coating and electroplating.

The tribological wear of mining machinery and equipment depends on the roughness and hardness of the surface. When roughness is low, the level of wear is mainly affected by adhesion. With increasing roughness of a metal element and increasing share of micro-cutting, abrasive wear becomes the dominant mechanism **[L. 15]**. In work **[L. 16]**, the authors showed that the wear intensity depends on the original properties of test materials and operating conditions. The test parameters also affect the tribological properties of the tested systems **[L. 17]**. Research results indicate that surfaces treated with different methods may have a similar surface geometry structure and significantly different friction coefficients **[L. 18]**. As a result of the technological transformation of the surface layer into the active layer under friction, extensive damage can usually be observed on the friction pair surfaces in the contact area that change the structure of the surface **[L. 19]**.

The addition of rare earth oxides (La_2O_3, Gd_2O_3, Lu_2O_3) improves the bulk Si3N4 material hardness **[L. 20]**. As reported in **[L. 21]**, rare earth oxides lower the friction coefficient and wear. Silicon nitride ceramics sintered with rare earth oxides are also an important class of materials for high-temperature applications as it exhibits good resistance to high temperatures, thermal shock, creep and high resistance to oxidation **[L. 20, 22, 23]**.

Pad welding of wear-resistant layers is a process that requires the selection of appropriate process parameters and materials. In this article, the authors demonstrate that modification effects vary depending on the materials used. Under the influence of high temperatures of welding techniques, metallurgical processes in the created layers shape the microstructure. The outer layers may mix with the buffer layers to some extent, thereby noticeably affecting the microstructure of the padded layers. As shown in previous works **[L. 3–5]**, adding rare earth metals into cast steel leads to the fragmentation of the microstructure, changes in the morphology and dispersion of non-metallic inclusions, which directly improves mechanical properties.

The authors present the beneficial effects of yttrium oxide Y_2O_3, cerium oxide Ce_2O_3 and lanthanum oxide La_2O_3 on the microstructure and selected tribological properties of paddings made with metallic powders.

MATERIALS AND METHODS

MIG/PAW pad welding process was used to manufacture the paddings. The padding weld had a base layer (buffer) and a wear-resistant working layer. The active layer was made from binders doped with cerium, yttrium and lanthanum oxides. The chemical composition of the consumables used is given in **Table 1.** The first series of paddings were manufactured on Hardox steel with a surface layer of 316L; the second and third series included the paddings on the S355 steel with the 55PTA padding, **Table 2.**

The produced padding weld variants were subjected to microstructure observations, hardness tests, tribological tests and the observations of the wear track surface geometry. Three tribological tests (reciprocating motion) were performed for each padding weld. The tribological system used is shown in **Figure 1.**

Table 1. Chemical composition of the consumables used
Tabela 1. Skład chemiczny zastosowanych materiałów spawalniczych

Consumable*	Chemical composition							
	C	Cr	**Ni**	**Mo**	**Mn**	**Fe**	**Si**	**Ti**
316L **	0.1	18	14	3	2	remainder	–	–
55PTA**	0.6	11	remainder	–	–	3	3.8	–
307**	0.08	19	9	–	7	remainder	0.8	–
46G***	0.2	6		3.5	0.9	remainder	0.5	0.25

* Manufacturer (** Capilla® Welding Materials GmbH, *** Welding Alloys)

Table 2. Variants of the padding welds prepared for testing
Tabela 2. Zestawienie wariantów wykonanych napoin

Sample	Material	Interlayer	Padding material	Additive
1-1	hardox	307	316L	–
1-2	hardox	307	316L	CeO_2
1-3	hardox	307	316L	La_2O_3
1-4	hardox	307	316L	Y_2O_3
2-1	S355	307	55PTA	–
2-2	S355	307	55PTA	CeO_2
2-3	S355	307	55PTA	La_2O_3
2-4	S355	307	55PTA	Y_2O_3
3-1	S355	46G	55PTA	–
3-2	S355	46G	55PTA	CeO_2
3-3	S355	46G	55PTA	La_2O_3
3-4	S355	46G	55PTA	Y_2O_3

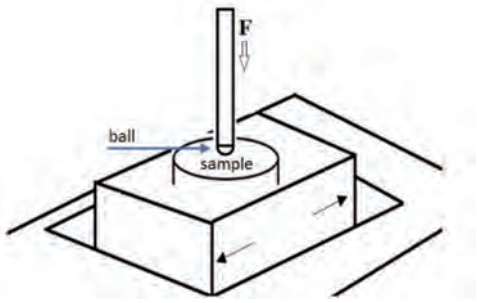

Fig. 1. Tribological system
Rys. 1. Węzeł tarcia

Table 3. Test equipment and parameters
Tabela 3. Urządzenia badawcze oraz parametry prowadzenia testów

Test type	Device	Test parameters
Micro-structure	Phenom XL	BSD Magnification x290, x1000
Hardness	NEXUS 4000	Nominal loading force: 10 kgf Indenter: Vickers
Tribo-logical tests	Anton Paar Tribometer TRB^3	Reciprocating motion Dry friction Amplitude: 10 mm Frequency: 1 Hz No of cycles: 10000 Path: 200 m Temperature: 23 ±1°C Humidity: 50 ±1%
Surface geometry structure	Leica DCM8	Confocal mode Lens x20 Max depth wear track area measured in a cross-section

RESULTS

The hardness of the components of mining machines and devices is one of the determining material properties.

Three hardness measurements of each padding were carried out in the three variants. Averaged measurement results are summarised in **Table 4**. No significant changes in hardness were observed during the first series of measurements. The highest increase in hardness was recorded for the Y_2O_3 – doped paddings.

A nearly 47% increase, compared with the reference padding, was observed in series two samples. Hardness measured on series three samples was about 65% higher than in the first series. The hardness of the paddings containing CeO_2 and La_2O_3 increased by 7%.

Table 4. Hardness test results
Tabela 4. Wyniki badań twardości napoin

Sample Designation	RE oxygen	Vickers hardness **HV 10**
1-1	–	187
1-2	**CeO_2**	184
1-3	**La_2O_3**	199
1-4	Y_2O_3	196
2-1	–	344
2-2	**CeO_2**	336
2-3	**La_2O_3**	304
2-4	**Y_2O_3**	369
3-1	–	335
3-2	CeO_2	353
3-3	**La_2O_3**	359
3-4	Y_2O_3	570

Microscopic observations of the paddings showed that the addition of rare earth metal oxides affected the microstructure. No significant changes in series 1 indicate a minor influence of rare earth oxides. This might be due to choosing the wrong consumable or incorrectly conducting the pad welding process (**Fig. 2**). Partial changes in the microstructures of the padding welds observed in series two samples (**Fig. 3**), such as different crystal arrangements and the change of individual regions of the existing phases, correspond directly to the test results of tribological properties. In series 3, the fragmentation of crystallisation crystals was mainly noted. No significant changes in properties were noted in the case of lanthanum oxide, where the microstructure has a similar appearance to that of the unmodified padding weld (**Fig. 4**).

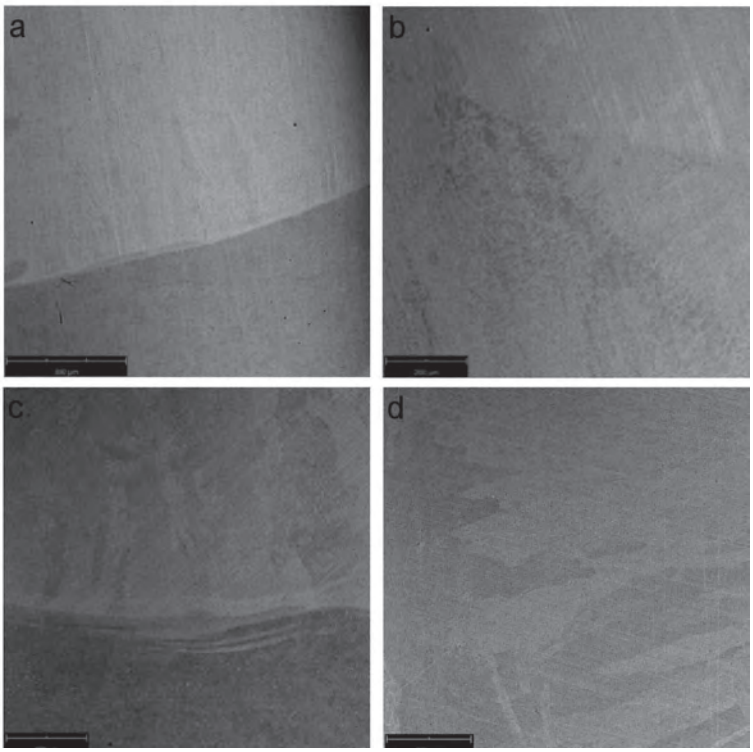

Fig. 2. Microstructure of the padding welds for series 1: a) non-modified, b) modified with CeO_2, c) La_2O_3, d) Y_2O_3
Rys. 2. Mikrostruktura napoin dla serii 1: a) bez dodatków RE oxides, b) CeO_2, c) La_2O_3, d) Y_2O_3

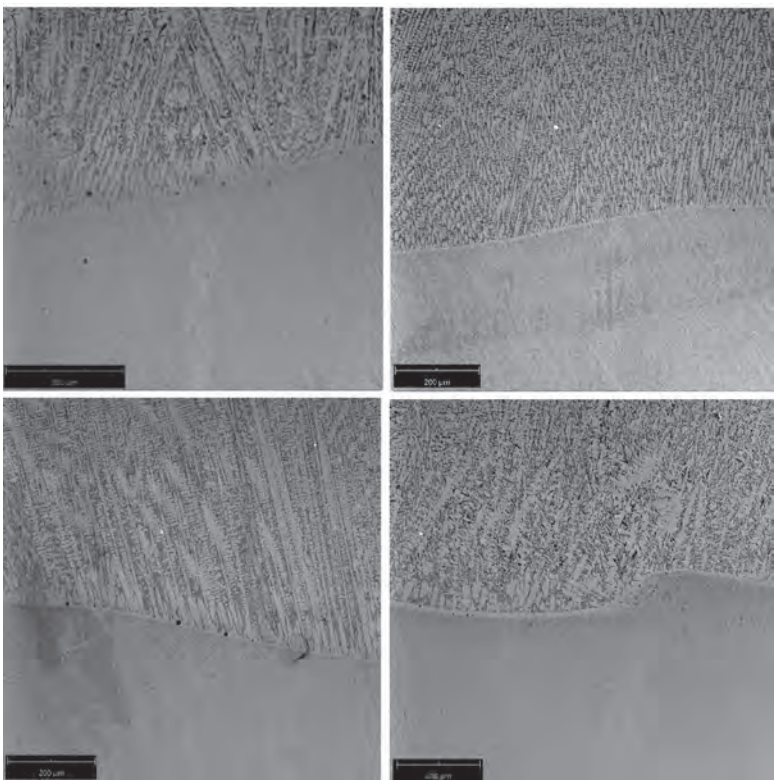

Fig. 3. Microstructure of the padding welds for series 2: a) non-modified, b) modified with CeO_2, c) La_2O_3, d) Y_2O_3
Rys. 3. Mikrostruktura napoin dla serii 2: a) bez dodatków RE oxides, b) CeO_2, c) La_2O_3, d) Y_2O_3

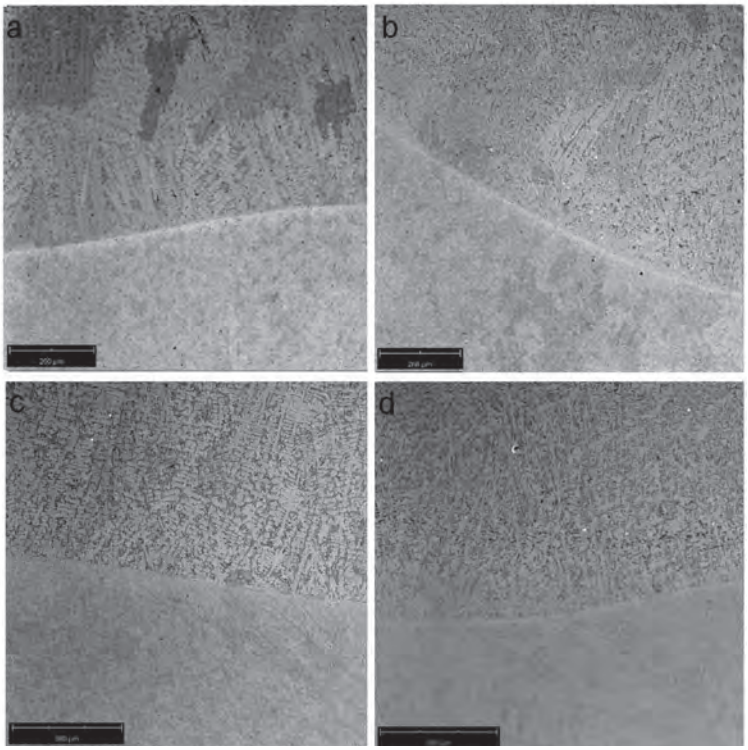

Fig. 4. Microstructure of the padding welds for series 3: a) non-modified, b) modified with CeO_2, c) La_2O_3, d) Y_2O_3
Rys. 4. Mikrostruktura napoin dla serii 3: a) bez dodatków RE oxides, b) CeO_2, c) La_2O_3, d) Y_2O_3

The increasing requirements for mining machines and devices force the multi-parameter assessment of tribological properties. Therefore, friction characteristics should be prepared based on a comprehensive analysis of the parameters recorded during the implementation of tribological tests – friction coefficients and data obtained from the tests of wear tracks – maximum wear depth and area.

During the operation of tribological systems with paddings on working components, friction and accompanying processes play a decisive role. Intense abrasive wear occurs in such systems due to the impact of loose particles on the material surface, causing fatigue, decohesion and material losses characteristic of abrasive wear. **Table 5** summarises the values of the mean friction coefficients μ obtained during the cooperation of the friction pairs under test.

The tests show that the lowest friction coefficients recorded under dry friction were recorded for the samples with the coating from series 3. It was found that in all the tested tribological systems, the 46G buffer layer reduced the resistance to motion. The highest efficiency was obtained for

Table 5. Tribological test results
Tabela 5. Wyniki badań tribologicznych

Sample Designation	RE oxygen	Coefficient of friction
1-1	–	0.60
1-2	**CeO_2**	0.55
1-3	**La_2O_3**	0.48
1-4	**Y_2O_3**	0.57
2-1	–	0.78
2-2	**CeO_2**	0.82
2-3	**La_2O_3**	0.54
2-4	**Y_2O_3**	0.79
3-1	–	0.67
3-2	**CeO_2**	0.38
3-3	**La_2O_3**	0.27
3-4	Y_2O_3	0.69

the coating with the addition of La_2O_3. The result of the cooperation of elements sliding against each other is tribological wear, which largely depends on the stereometric properties of the surfaces of the triboelements. After tribological tests, microscopic observations of the surfaces were performed. The isometric images and wear profiles from the cross-section are shown in **Figures 5–7**. The maximum wear depth and the wear surface area were assumed as the measure of wear. **Figure 8** shows the values of the maximum wear track depth, and **Figure 9** shows the values of the wear track area.

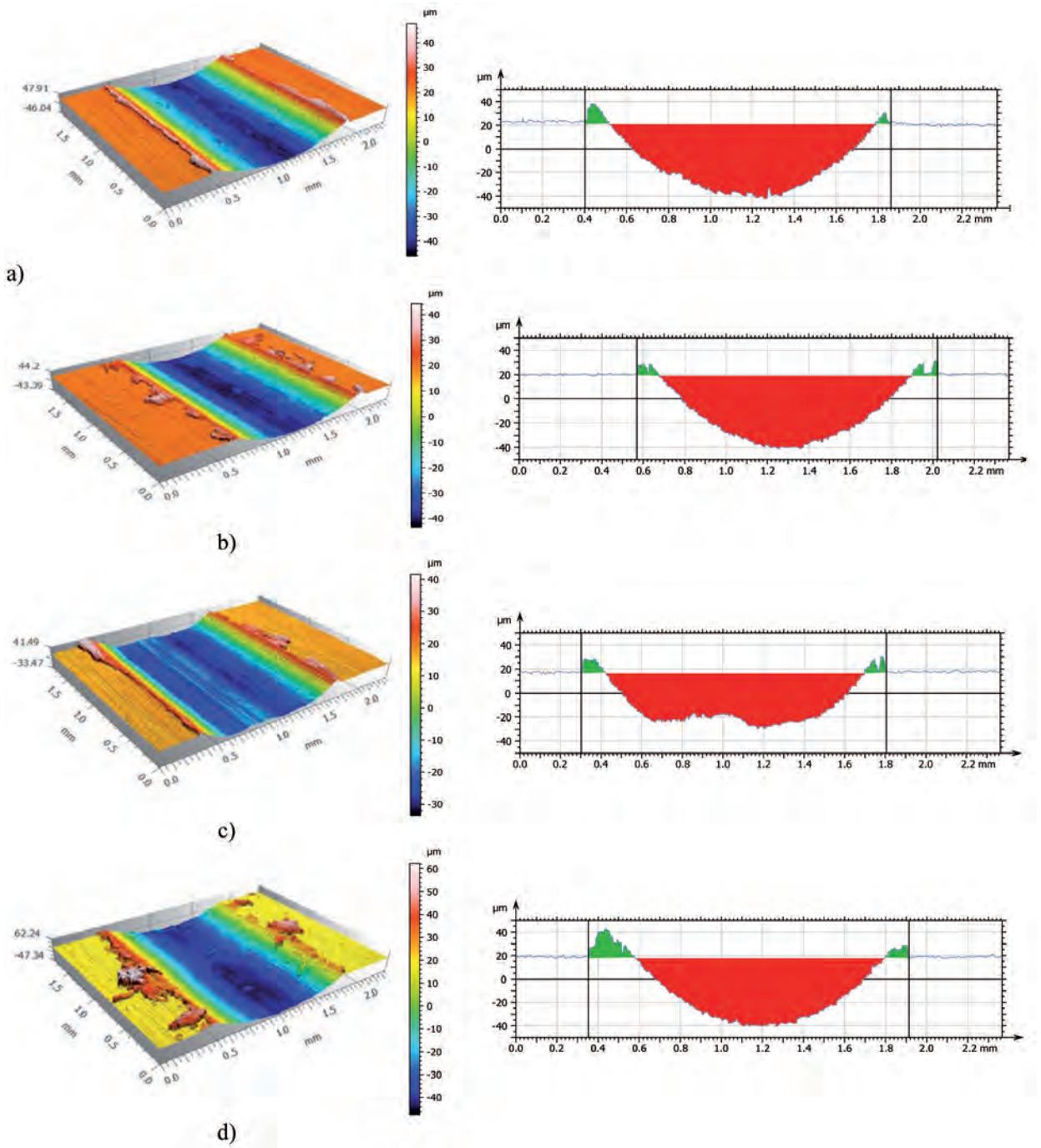

Fig. 5. Isometric images and cross-sectional area profiles for wear tracks in series 1: a) non-modified, b) modified with CeO_2, c) La_2O_3, d) Y_2O_3

Rys. 5. Obrazy izometryczne i profile śladów wytarcia na przekroju poprzecznym dla serii 1: a) bez dodatków RE oxides, b) CeO_2, c) La_2O_3, d) Y_2O_3

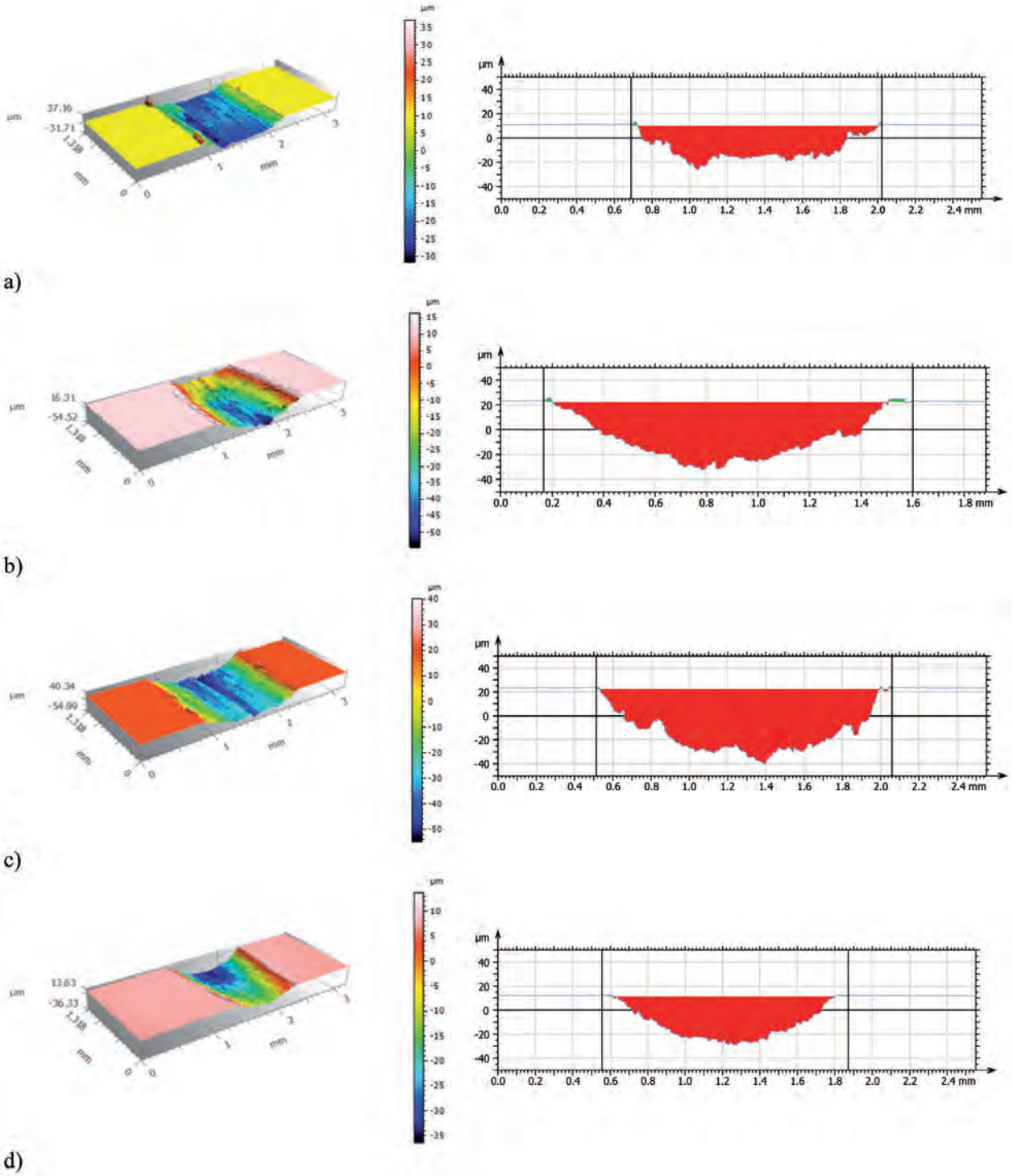

Fig. 6. Isometric images and cross-sectional area profiles for wear tracks in series 2: a) non-modified, b) modified with CeO_2, c) La_2O_3, d) Y_2O_3

Rys. 6. Obrazy izometryczne i profile śladów wytarcia na przekroju poprzecznym dla serii 2: a) bez dodatków RE oxides, b) CeO_2, c) La_2O_3, d) Y_2O_3

The isometric images in **Figures 5–7** indicate the abrasive wear mechanism of the tested samples. For the first series – iron-based padding welds – characteristic damming was observed at the edges of the wear track. Comparative analysis of the wear profiles on cross-sections after dry friction shows that the surface with the Y_2O_3-modified nickel-based padding had the highest application efficiency – the lowest wear. The wear track depth value was two times smaller, and the wear track area

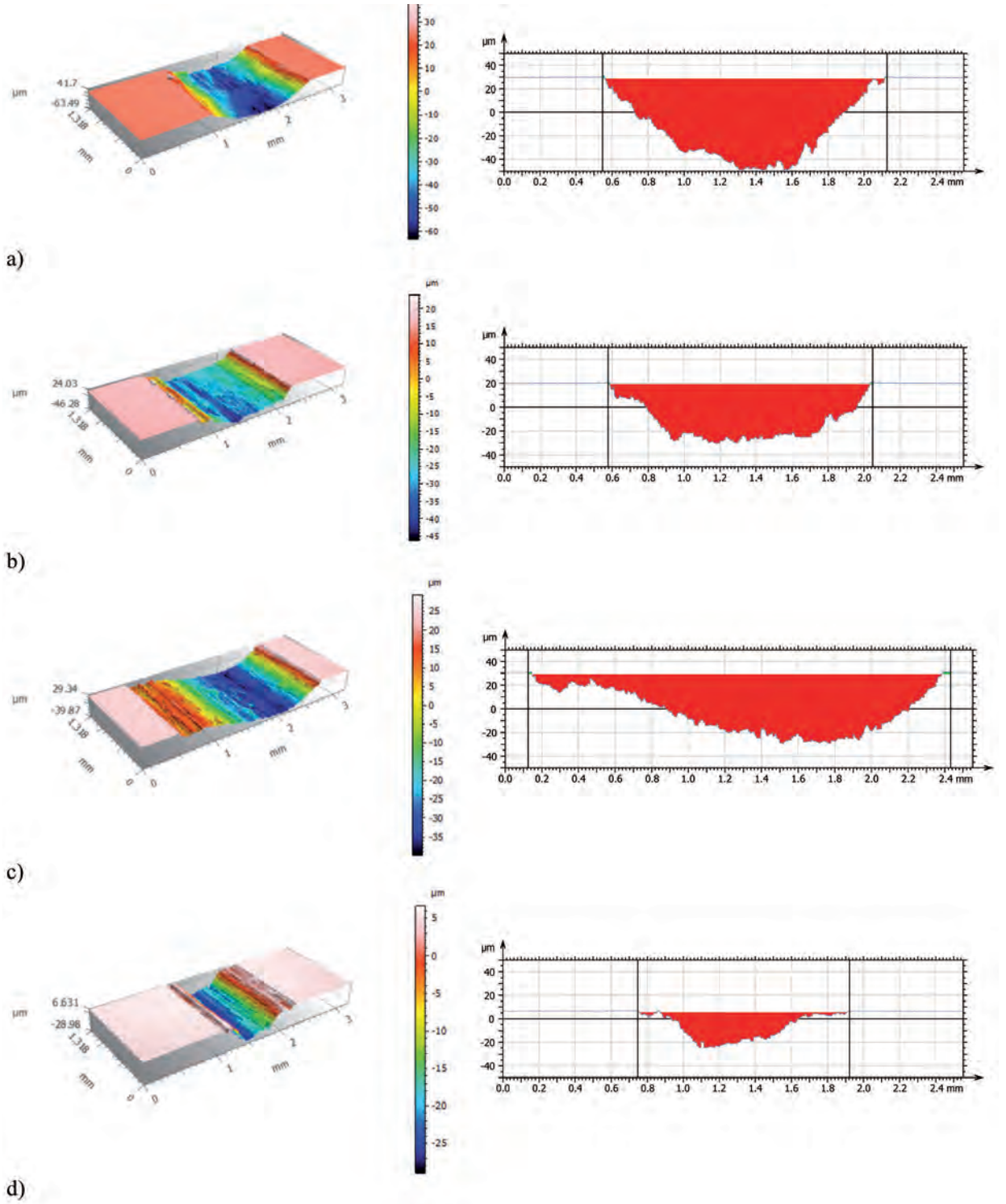

Fig. 7. Isometric images and cross-sectional area profiles for wear tracks in series 3: a) non-modified, b) modified with CeO_2, c) La_2O_3, d) Y_2O_3

Rys. 7. Obrazy izometryczne i profile śladów wytarcia na przekroju poprzecznym dla serii 3: a) bez dodatków RE oxides, b) CeO_2, c) La_2O_3, d) Y_2O_3

recorded for this padding was 4.5 times smaller. For the La_2O_3 – containing paddings, an increase in hardness was about 40%, with a simultaneous reduction in friction coefficient of more than 43% for padding welds with a nickel matrix and the 46G buffer layer. For series 2, the lowest maximum wear track depth was recorded for the unmodified padding weld.

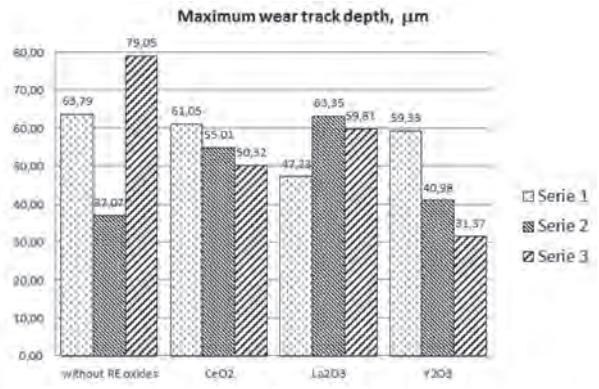

Fig. 8. Cross-section of the maximum wear track depth
Rys. 8. Maksymalna głębokość wytarcia na przekroju poprzecznym [µm]

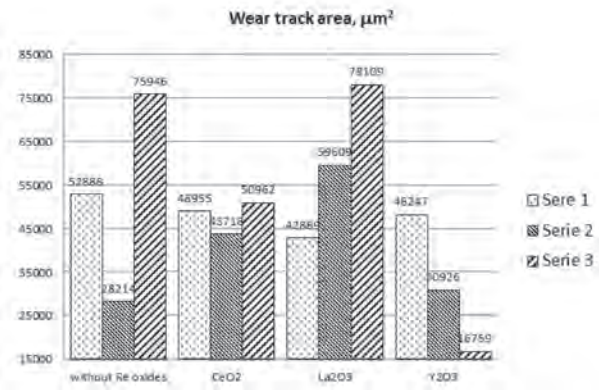

Fig. 9. Cross-section of the wear track area
Rys. 9. Pole powierzchni wytarcia na przekroju poprzecznym [µm^2]

In contrast, series 3 shows significant changes in the modified samples. Smaller values of the maximum wear track depth were recorded compared to the padding weld without the addition of the modifier. The evaluation of the abrasion field for series 2 indicates significant wear of the modified surfacing welds, and the most favourable effect of modifiers was observed for series 3.

CONCLUSIONS

This study showed that rare earth metal oxides could be used in padding weld manufacture. The microstructural changes in the oxides allow for controlling the increase in hardness and effective reduction of friction coefficient. It should be noted, however, that the results will vary depending on the material used. Therefore, the material selection for paddings should rely on the tests for the relationship between surface hardness and roughness and tribological properties of the systems under analysis. As a result of the conducted friction tests, different tribological characteristics were obtained depending on the type of base materials, the buffer layer and the type of rare earth metal oxide. Tribological tests found that yttrium oxide had the most favourable effect on nickel-based and 46G buffer layers. Nearly all modification cases with rare earth oxides reduced the maximum wear track depth and area. In the case of hard and wear-resistant paddings with significantly large dimensions (up to 8 mm), the interpretation of the modification results is not that clear. Many variables, such as the chemical composition of the materials used, their mechanical properties, technological processes and testing conditions, could affect the wear processes. Analysis of the results of tribological tests of paddings modified with oxides of rare earth metals shows the influence of the technology used on the improvement of tribological properties of the tested systems. These processes contributed to lower motion resistance and wear rates compared to unmodified samples.

REFERENCES

1. Naumov A.V.: Review of the world market of rare earth metals. Russian Journal of Non–Ferrous Metals 2008, 49(1), pp. 22–31.
2. Longmei Wang, Qin Lin, Jingwen Ji, Denian Lan: New study concerning development of application of rare earth metals. Journal of Alloys and Compounds 2005, 408–412, pp. 384–386.
3. Kasińska J.: Wide-ranging influence of mischmetal on properties of G17CrMo5-5 cast steel. Metalurgija 2015, 54 (1), pp. 135–138.
4. Kasińska J.: Influence of Rare Earth Metals on Microstructure and Mechanical Properties of G20Mn5 Cast Steel. Archives of Foundry Engineering 2018, (3), pp. 37–42.

5. Kasińska J., Myszka D.: Influence of rare earths metals (REM) on the structure and selected properties of grey cast iron. Metalurgija 2020, 59 (4), pp. 459–462.
6. Wang K.L., Zhang Q.B., Sun M.L., Wei X.G., Zhu Y.M.: Microstructure and corrosion resistance of laser clad coatings with rare earth elements. Corrosion Science 2001, 43, pp. 255–267.
7. Wang X.H., Zhang M., Zhou Z.D., Qu S.Y.: Microstructure and properties of laser clad TiC+ NiCrBSi+ rare earth composite coatings. Surface and Coatings Technology 2002, 161, pp. 195–199.
8. Zhao G.M., Wang K.L.: Effect of La2O3 on corrosion resistance of laser clad ferrite-based alloy coatings. Corrosion Science 2006, 48, pp. 273–284.
9. Liu Q.B., Zou J.L., Zheng M., Dong C.: Effect of Y2O3 content on microstructure of gradient bioceramic composite coating produced by wide-band laser cladding. J. Rare Earths 2005, 23(4), p. 446.
10. Wu C.F., Ma M.X., Liu W.J., Zhong M.L., Zhang H.J., Zhang W.M.: Laser cladding in-situ carbide particle reinforced Fe-based composite coatings with rare earth oxide addition. J. Rare Earths 2009, 27(6), p. 997.
11. Yi W., Zheng C.Q., Fan P., Cheng S.H., Li W., Ying G.F.: Effect of rare earth on oxidation resistance of iron base fluxing alloy spray-welding coating. J. Alloys Compd. 2000, 311(1), p. 65.
12. Xing X.G., Han Z.J., Wang H.F., Lu P.N.: Electrochemical corrosion resistance of CeO2-Cr/Ti coatings on 304 stainless steel via pack cementation. J. Rare Earths 2015, 33(10), p. 1122.
13. Liu Y., Hang, Z., Yang G. et al.: Influence of Rare Earth on the High-Temperature Sliding Wear Behavior of WC-12Co Coating Prepared by HVOF Spraying. J Therm Spray Tech, 2018, 27, pp. 1143––1152.
14. Jin J., Sun J., Wang W., Song J., Xu H.: Effect of Rare Earth on Microstructure and Wear Resistance of In-Situ-Synthesized Mo2FeB2 Ceramics-Reinforced Fe-Based Cladding. Materials 2020, 13, p. 3633.
15. Nosal S.: Tribology. Introduction to the issues of friction, wear, and lubrication. Poznań 2012.
16. Stachowiak A., Tyczewski P., Zwierzycki W.: The application of wear maps for analyzing the results of research into tribocorrosion. Wear 2016, 352–353, pp. 146–154.
17. Woś S., Koszela W., Pawlus P., Sęp J.: The influence of research parameters on friction coefficients for the texturing of both sliding surfaces. Tribologia 2015, 46 (5), pp. 147–154.
18. Zawadzki P., Wierzbicka N., Talar R., Burysz Ł.: Tribological properties of hardened surfaces constituted by various methods of mechanical processing. Tribologia 2021, 4, pp. 57–72.
19. Kaczor G.: The effect of selected factors on the process of wear under oscillatory motion. Tribologia 2018, 3, pp. 51–58.
20. Satet R.L., Hoffmann M.J.: Experimental evidence of the impact of rare-earth elements on particle growth and mechanical behaviour of silicon nitride. J. Am. Ceram. Soc. 2000, 88 (9), pp. 2485–2490.
21. Tatarkoa P., Kasiarováa M., Dusza J., Morgielb J., Sajgalíkc P., Hvizdoˇs P.: Wear resistance of hot-pressed Si3N4/SiC micro/nanocomposites sintered with rare-earth oxide additives. Wear 2010, 269, pp. 867–874.
22. Becher P.F., Painter G.S., Shibata N., Waters S.B., Lin H.T.: Effects of rare-earth(RE) intergranular adsorption on the phase transformation, microstructureevolution, and mechanical properties in silicon nitride with RE2O3+MgOadditives: RE = La, Gd, and Lu. J. Am. Ceram. Soc. 2008, 91 (7), pp. 2328––2336.
23. Becher P.F., Shibata N., Painter G.S., Averill F., Van Benthem K., Lin H.-T., Waters S.B.: Observations on the influence of secondary Me oxide additives (Me = Si, Al, Mg) on the microstructural evolution and mechanical behavior of siliconnitride ceramics containing RE2O3(RE = La, Gd, Lu). J. Am. Ceram. Soc. 2010, 93 (2), pp. 570–580.